Journal of Solid State Chemistry **152,** 152–158 (2000)
doi:10.1006/jssc.2000.8681, available online at http://www.idealibrary.com on IDEAL®

A Pillared Three-Dimensional Manganese(II) Coordination Network Containing Rectangular Channels: Synthesis, X-Ray Structure, and Magnetic Properties

Wenbin Lin,*,[1] Owen R. Evans,* and Gordon T. Yee†

*Department of Chemistry, Brandeis University, Waltham, Massachusetts 02454; and †Department of Chemistry and Biochemistry, University of Colorado, Boulder, Colorado 80309

An unusual pillared 3-D manganese(II) coordination network based on carboxylate-bridged trimanganese cores $[Mn_6(isonicotinate)_{10}(H_2O)_2](ClO_4)_2(EtOH)_2(H_2O)_3$, 1, was synthesized by treating manganese(II) perchlorate and 4-pyridinecarboxyaldehyde under hydro(solvo)thermal conditions. A single crystal X-ray diffraction study revealed that 1 contains rectangular channels that are occupied by perchlorate counterions and disordered ethanol and water guest molecules. The included ethanol and water guest molecules as well as the coordinated water molecules can be removed under vacuum at room temperature to afford a nanoporous solid that maintains the framework structure of 1. Magnetic measurements indicate antiferromagnetic interactions among the high-spin Mn(II) centers in 1 with coupling constants of −3.08 K and −4.96 K for the roughly isosceles triangular trimanganese cluster. Crystal data for 1: $C_{64}H_{62}Cl_2Mn_6N_{10}O_{35}$, monoclinic space group $P2_1/n$, $a = 18.7892(3)$ Å, $b = 23.2307(1)$ Å, $c = 21.1355(4)$ Å, $B = 95.085(1)^\circ$, $Z = 4$, $R1 = 0.0719$, $_wR2 = 0.261$, and Goo$F = 1.02$. © 2000 Academic Press

INTRODUCTION

The synthesis of polymeric coordination networks has witnessed significant progress over the past few years, in part motivated by the prospect of generating new materials with interesting structures and exploitable functions (1). The research on nanoporous coordination polymers has been particularly fruitful, and now many solids containing potentially useful nanopores have become available (2). The design of coordination networks with active functional properties is far more difficult owing to the stringent requirements placed upon both the metal centers and the linking ligands as well as their spatial arrangements (3). For example, the polar orientation of electronically unsymmetrical chromophoric building blocks is a prerequisite for the observation of bulk second-order NLO properties, which presents a particular challenge for synthetic chemists (4). We have recently demonstrated the feasibility of the rational synthesis of NLO-active polar solids based on 2D and 3D Zn^{II} and Cd^{II} polymeric coordination networks containing electronically unsymmetrical pyridinecarboxylate ligands with the carboxylate functionality in either monodentate or chelating binding mode (5). In view of typically negligible absorption for the $d \rightarrow d$ transitions in Mn(II) centers, we have examined the reaction between manganese(II) perchlorate and 4-pyridinecarboxaldehyde in the hope of generating a transparent acentric Mn(II) coordination polymer. Herein we wish to report the synthesis of an unusual pillared 3D manganese(II) coordination network based on carboxylate-bridged trimanganese cores, $[Mn_6(isonicotinate)_{10}(H_2O)_2](ClO_4)_2(EtOH)_2(H_2O)_3$, **1**. Owing to the bridging nature of the carboxylate groups, **1** is centrosymmetric and does not exhibit second-order optical nonlinearity. The X-ray crystal structure of **1** reveals the presence of rectangular open channels that are occupied by perchlorate counterions and disordered ethanol and water guest molecules. The nanoporosity and magnetic properties of **1** are also described in this paper.

EXPERIMENTAL

Materials and Methods

All chemicals were purchased from Aldrich, and used without further purification. The IR spectra were recorded as KBr pellets on a Perkin-Elmer Paragon 1000 FT-IR spectrometer. X-ray powder diffraction data (XRPD) were recorded on a Rigaku RU300 diffractometer at 60 kV, 300 mA for Cu$K\alpha$ ($\lambda = 1.5418$ Å), with a scan speed of 2°/min and a step size of 0.02° in 2θ. The calculated XRPD patterns were produced using the SHELXTL-XPOW program and single crystal reflection data. TGA experiments were carried out with a Shimadzu

[1]To whom correspondence should be addressed. E-mail: wlin@brandeis.edu.

0022-4596/00 $35.00

TGA-50 TG analyzer at a heating rate of 15°C/min under nitrogen.

Magnetization vs temperature data were obtained on a Quantum Design MPMS-5S SQUID magnetometer in 100 G applied field. Approximately 15 mg of **1** was loaded between two cotton plugs in a gelatin capsule. A diamagnetic correction for the sample was calculated from Pascal's constants. The correction for the capsule and the cotton was calculated from the measured average gram susceptibility of several nominally identical empty capsules and cotton plugs.

Synthesis of $[Mn_3(isonicotinate)_5(H_2O)][ClO_4]\cdot(EtOH)(H_2O)_{1.5}$, **1**. A mixture of $Mn(ClO_4)_2\cdot 6H_2O$ (0.181 g, 0.5 mmol) and 4-pyridinecarboxyaldehyde (0.107 g, 1.0 mmol) was thoroughly mixed with ethanol (0.3 mL) and H_2O (0.1 mL) in a heavy-walled pyrex tube. The tube was frozen with liquid nitrogen and sealed under vacuum. After heated in an oven at 100°C for 72 h, pale yellow prismatic crystals were obtained. Yield: 0.15 g (93%). IR (cm^{-1}): 3366 (br), 2969 (w), 1636 (s), 1552 (s), 1499 (w), 1388 (s), 1228 (w), 1081 (br, s), 1016 (w), 866 (w), 773 (m), 710 (w), 688 (s), 624 (w), 564 (w).

Removal of guest molecules. A sample of freshly prepared **1** (221 mg) was ground and subjected to 0.01 Torr vacuum at room temperature. After 24 h, the sample experienced a weight loss of 23.6 mg (10.7%) and no further weight loss could be observed. This weight loss corresponded to the removal of all the guest ethanol and water molecules as well as the coordinated water molecules (calcd. 9.43%). X-ray powder diffraction pattern taken immediately after the removal of guest molecules indicated that the resulting nanoporous solid maintained the framework structure of **1**.

X-ray data collections and structure determination. Data collection for **1** was carried out with a colorless crystal of dimensions of $0.15\times0.17\times0.38$ mm on a Siemens SMART system equipped with a CCD detector using Mo$K\alpha$ radiation. Of the 21,944 unique reflections measured, 11,915 reflections with $I > 2\sigma(I)$ were used in structure solution and refinement. The structure was solved by direct methods (6) and refined (7) on F^2 by full-matrix least squares using anisotropic displacement parameters for all nonhydrogen atoms on the manganese isonicotinate framework and the chlorine atoms of the perchlorate anions. Due to the severe disorder problem of the water and ethanol guest molecules and one of the two perchlorate anions, their oxygen and carbon atoms were located in electron density maps and refined using isotropic displacement parameters. The locations of disordered perchlorate anion and ethanol and water guest molecules are only approximate. All the hydrogen atoms for the isonicotinate groups were located by geometric placing. No attempts were made to locate the hydrogen atoms on the water and ethanol molecules. Final refinement gave an $R1 = 0.0719$, ${}_wR2 = 0.261$, and goodness of fit = 1.02. Experimental details for X-ray data collections of **1** are tabulated in Table 1. Atomic coordinates of **1** are listed in Table 2, while selected bond distances and angles for **1** are listed in Table 3. All bond distances and angles for the isonicotinate groups are normal and not listed in Table 3.

TABLE 1
Crystallographic Data of 1

Chemical formula	$C_{64}H_{62}Cl_2Mn_6N_{10}O_{35}$
Crystal system	Monoclinic
Space Group	$P2_1/n$ (No. 14)
a (Å)	18.7892 (3)
b (Å)	23.2307 (1)
c (Å)	21.1355 (4)
β (°)	95.085 (1)
V (Å^3)	9189.2 (2)
Z	4
Formula Wt	1931.76
T (K)	123 (2)
λ (Mo$K\alpha$) (Å)	0.71073
ρ_{calc} (g/cm^3)	1.396
μ (cm^{-1}) (Mo$K\alpha$)	9.4
N_{ref} (total)	21944
N_{ref} (obs.), $I > 2\sigma(I)$	11915
N_{par}	1013
$R1$	0.0719
${}_wR2$	0.261
Goodness of fit	1.02
Min. and max. residual density (e/Å^3)	−1.51, 2.37

RESULTS AND DISCUSSION

Compound **1** was obtained as large pale yellow rod-like crystals in 93% yield by a hydro(solvo)thermal reaction between $Mn(ClO_4)_2\cdot 6H_2O$ and 4-pyridinecarboxaldehyde in a mixture of ethanol and water at 100°C. The IR spectrum of **1** exhibits peaks at 1552 and 1388 cm^{-1} that can be assigned to the antisymmetric and symmetric C=O stretches, respectively. The absence of an aldehydic carbonyl peak (1680–1720 cm^{-1}) in the FT-IR spectra indicates that the isonicotinate group has resulted from the slow oxidation of 4-pyridinecarboxaldehye under the reaction conditions (8). Bulk purity was ensured via comparison of the XRPD pattern of **1** with a calculated XRPD pattern obtained from single crystal reflection data.

Compound **1** crystallizes in the monoclinic space group $P2_1/n$. The asymmetric unit consists of 6 Mn(II) centers, 10 bridging isonicotinate groups, 2 coordinated water molecules, 2 perchlorate anions, and 3 water and 2 ethanol guest molecules (Fig. 1). The asymmetric unit contains two crystallographically inequivalent $[Mn_3(isonicotinate)_5(H_2O)]^+$ building blocks that are composed of Mn1, Mn2, and Mn3 centers and Mn4, Mn5, and Mn6 centers, respectively

TABLE 2
Fractional Atomic Coordinates and Isotropic Displacement Parameters of 1

Atom	*x*	*y*	*z*	U_{eq} (Å^2)
Mn1	0.16197(4)	0.88138(3)	0.34316(4)	0.0095(2)
Mn2	0.26885(4)	0.87838(3)	0.16902(4)	0.0105(2)
Mn3	0.20685(4)	1.00620(3)	0.24693(4)	0.0108(2)
Mn4	0.70725(4)	0.74936(3)	0.25895(4)	0.0116(2)
Mn5	0.66257(4)	0.88231(3)	0.34137(4)	0.0099(2)
Mn6	0.76902(4)	0.86790(3)	0.16734(4)	0.0103(2)
O1	0.27741(19)	0.89541(16)	0.34485(17)	0.0139(11)
O2	0.29460(18)	0.94114(15)	0.25373(16)	0.0107(11)
O3	0.2611(2)	0.80927(15)	0.23194(18)	0.0161(12)
O4	0.1725(2)	0.80061(16)	0.29597(18)	0.0154(12)
O5	0.65337(19)	0.86443(16)	0.15746(17)	0.0148(11)
O6	0.63935(19)	0.82804(15)	0.25415(16)	0.0124(11)
O7	0.75775(19)	0.94635(15)	0.21656(17)	0.0140(11)
O8	0.67225(19)	0.95691(16)	0.28424(18)	0.0151(11)
O9	0.65349(19)	0.81135(16)	0.40519(17)	0.0155(12)
O10	0.7211(2)	0.74744(16)	0.35811(17)	0.0192(11)
O11	0.2064(2)	1.01283(16)	0.14648(17)	0.0171(12)
O12	0.2807(2)	0.94839(16)	0.10817(17)	0.0179(12)
O13	0.77702(19)	0.86723(16)	0.34429(17)	0.0159(11)
O14	0.79557(19)	0.81291(15)	0.25914(16)	0.0118(11)
O15	0.13723(18)	0.92896(15)	0.25153(16)	0.0108(10)
O16	0.1528(2)	0.88377(16)	0.15972(17)	0.0159(12)
O17	0.6951(2)	0.73614(16)	0.16004(18)	0.0206(12)
O18	0.7778(2)	0.78942(16)	0.11721(18)	0.0177(12)
O19	0.2242(2)	1.01584(16)	0.34631(17)	0.0190(12)
O20	0.1549(2)	0.95755(16)	0.39918(17)	0.0154(11)
O21	0.6053(2)	0.70213(17)	0.2600(2)	0.0236(14)
O22	0.1048(2)	1.05328(17)	0.2412(2)	0.0256(14)
N1	0.5448(2)	0.90275(19)	0.3443(2)	0.0140(12)
N2	0.2432(3)	0.5970(2)	0.2524(2)	0.0188(16)
N3	0.3874(2)	0.86128(19)	0.1688(2)	0.0133(12)
N4	0.7399(3)	1.15956(19)	0.2350(2)	0.0189(16)
N5	0.7472(2)	0.6791(2)	0.5815(2)	0.0178(16)
N6	0.2410(2)	1.0878(2)	− 0.0710(2)	0.0162(14)
N7	1.0443(2)	0.86176(19)	0.3463(2)	0.0137(12)
N8	− 0.1128(2)	0.88330(19)	0.1694(2)	0.0133(12)
N9	0.6856(2)	0.66393(19)	− 0.0636(2)	0.0156(12)
N10	0.3019(2)	1.0641(2)	0.5715(2)	0.0157(12)
C1	0.5144(3)	0.9456(2)	0.3070(3)	0.0152(17)
C2	0.4412(3)	0.9521(2)	0.2951(3)	0.0145(17)
C3	0.4998(3)	0.8667(2)	0.3710(3)	0.0154(17)
C4	0.4263(3)	0.8717(2)	0.3619(3)	0.0178(17)
C5	0.3958(3)	0.9139(2)	0.3220(2)	0.0108(16)
C6	0.3162(3)	0.9169(2)	0.3069(2)	0.0122(17)
C7	0.2087(3)	0.6216(3)	0.2979(3)	0.0239(19)
C8	0.1971(3)	0.6797(2)	0.3018(3)	0.0197(17)
C9	0.2681(3)	0.6328(2)	0.2090(3)	0.0204(19)
C10	0.2614(3)	0.6915(2)	0.2111(3)	0.0194(17)
C11	0.2259(3)	0.7162(2)	0.2587(3)	0.0152(17)
C12	0.2190(3)	0.7807(2)	0.2624(2)	0.0138(17)
C13	0.4190(3)	0.8206(2)	0.2067(3)	0.0168(17)
C14	0.4920(3)	0.8149(2)	0.2180(3)	0.0158(17)
C15	0.4310(3)	0.8962(3)	0.1385(3)	0.0188(17)
C16	0.5036(3)	0.8921(3)	0.1454(3)	0.0192(17)
C17	0.5357(3)	0.8519(2)	0.1870(2)	0.0123(17)
C18	0.6155(3)	0.8482(2)	0.2002(2)	0.0119(17)
C19	0.7047(3)	1.1355(2)	0.2812(3)	0.0218(17)
C20	0.6943(3)	1.0766(2)	0.2853(3)	0.0211(17)
C21	0.7639(3)	1.1239(2)	0.1919(3)	0.0213(19)
C22	0.7569(3)	1.0657(2)	0.1938(3)	0.0196(17)
C23	0.7220(3)	1.0406(2)	0.2420(3)	0.0147(17)
C24	0.7161(3)	0.9757(2)	0.2477(2)	0.0117(17)
C25	0.6943(3)	0.7180(2)	0.5757(3)	0.0193(17)
C26	0.6746(3)	0.7477(2)	0.5204(3)	0.0183(17)
C27	0.7831(3)	0.6699(3)	0.5306(3)	0.0226(17)
C28	0.7677(3)	0.6975(3)	0.4735(3)	0.0242(17)
C29	0.7117(3)	0.7371(2)	0.4678(2)	0.0139(17)
C30	0.6935(3)	0.7678(2)	0.4052(2)	0.0123(17)
C31	0.1985(3)	1.1035(3)	− 0.0249(3)	0.0195(17)
C32	0.1987(3)	1.0748(2)	0.0318(3)	0.0175(17)
C33	0.2850(3)	1.0416(3)	− 0.0588(3)	0.0204(17)
C34	0.2868(3)	1.0110(2)	− 0.0033(3)	0.0184(17)
C35	0.2426(3)	1.0270(2)	0.0434(2)	0.0143(17)
C36	0.2431(3)	0.9935(2)	0.1039(3)	0.0155(17)
C37	0.9977(3)	0.9001(2)	0.3677(2)	0.0151(17)
C38	0.9248(3)	0.8940(2)	0.3592(3)	0.0180(17)
C39	1.0154(3)	0.8143(2)	0.3163(3)	0.0168(17)
C40	0.9427(3)	0.8066(2)	0.3039(3)	0.0166(17)
C41	0.8956(3)	0.8473(2)	0.3252(2)	0.0109(17)
C42	0.8166(3)	0.8421(2)	0.3092(2)	0.0118(17)
C43	− 0.0689(3)	.8465(2)	0.1441(3)	0.0173(17)
C44	0.0050(3)	0.8524(2)	0.1504(3)	0.0174(17)
C45	− 0.0831(3)	0.9284(2)	0.2021(3)	0.0152(17)
C46	− 0.0104(3)	0.9367(2)	0.2131(3)	0.0148(17)
C47	0.0348(3)	0.8978(2)	0.1872(2)	0.0131(17)
C49	0.6509(3)	0.6504(2)	− 0.0126(3)	0.0176(17)
C50	0.6644(3)	0.6766(2)	0.0462(3)	0.0188(17)
C51	0.7371(3)	0.7051(3)	− 0.0553(3)	0.0197(17)
C52	0.7538(3)	0.7330(3)	0.0009(3)	0.0221(17)
C53	0.7159(3)	0.7195(2)	0.0529(3)	0.0168(17)
C54	0.7313(3)	0.7510(2)	0.1149(3)	0.0156(17)
C55	0.3261(3)	1.0774(3)	0.5141(3)	0.0216(17)
C56	0.2946(3)	1.0568(3)	0.4578(3)	0.0230(17)
C57	0.2466(3)	1.0277(2)	0.5712(3)	0.0183(17)
C58	0.2118(3)	1.0055(2)	0.5161(3)	0.0172(17)
C59	0.2365(3)	1.0195(2)	0.4574(3)	0.0155(17)
C60	0.2012(3)	0.9952(2)	0.3963(2)	0.0141(17)
Cl2	0.55562(13)	0.56755(9)	0.16105(12)	0.0645(9)
O29	0.4847(3)	0.5458(3)	0.1577(3)	0.0622(17)
O30	0.5870(5)	0.5449(4)	0.1050(4)	0.119(3)
O31	0.5561(3)	0.6307(3)	0.1561(3)	0.0638(17)
O32	0.5851(5)	0.5532(4)	0.2249(5)	0.135(3)
Cl1[a]	0.05220(14)	1.22010(12)	0.03135(14)	0.0442(11)
Cl3[a]	0.0535(7)	1.2003(4)	0.1319(6)	0.61(3)
O36	0.1123(5)	1.2261(4)	0.0838(4)	0.114(3)
O28[a]	− 0.0738(4)	1.1526(3)	0.1290(3)	0.059(2)
C65[a]	− 0.0652(10)	1.0836(8)	0.1130(8)	0.124(6)
C66[a]	− 0.1125(11)	1.0749(9)	0.0496(10)	0.144(7)
O23[a]	0.4324(17)	0.9319(13)	0.5301(14)	0.062(9)
C61[a]	0.3860(11)	0.8505(9)	0.5874(10)	0.100(5)
C62[a]	0.3695(17)	0.8965(13)	0.5364(14)	0.024(7)
O24	0.4304(7)	0.9124(6)	− 0.0298(6)	0.195(5)
C64	0.4405(18)	0.9401(14)	− 0.0998(17)	0.323(15)
O25	0.5087(9)	0.7988(7)	0.0078(8)	0.272(8)
O26	0.3731(11)	0.6635(8)	0.0269(9)	0.314(9)
O27	0.4440(12)	0.7141(9)	0.0764(10)	0.331(10)
O33[a]	− 0.0142(4)	1.2374(3)	0.0550(4)	0.049(3)
O34[a]	0.0497(5)	1.1612(4)	0.0190(4)	0.068(4)
O35[a]	0.0637(6)	1.2479(4)	− 0.0248(5)	0.085(5)
C63	0.5074(14)	0.9742(10)	− 0.0305(11)	0.229(11)
O37[a]	0.0798(5)	1.1620(4)	0.1965(4)	0.008(3)
O38[a]	0.004200	1.257900	0.157300	0.1000
O39[a]	− 0.008200	1.159000	0.085300	0.1000

TABLE 2—*Continued*

[a]Partial occupancies.

TABLE 3
Selected Bond Distances (Å) and Bond Angles (°) for 1

Mn1–O1	2.191(4)	Mn3–O22	2.201(4)
Mn1–O4	2.142(4)	Mn3–N2[a]	2.308(5)
Mn1–O15	2.243(3)	Mn6–O5	2.166(4)
Mn1–O20	2.140(4)	Mn6–O7	2.118(4)
Mn1–N7[b]	2.264(4)	Mn6–O14	2.340(3)
Mn1–N9[c]	2.244(4)	Mn6–O18	2.122(4)
Mn2–O2	2.326(3)	Mn6–N8[d]	2.246(4)
Mn2–O3	2.098(4)	Mn6–N6[e]	2.274(4)
Mn2–O12	2.098(4)	Mn2–O16	2.176(4)
Mn2–N3	2.263(4)	Mn2–N5[f]	2.288(4)
Mn5–O6	2.244(3)	Mn5–O8	2.129(4)
Mn5–O9	2.146(4)	Mn5–O13	2.174(4)
Mn5–N1	2.269(4)	Mn5–N10[g]	2.274(4)
Mn4–O6	2.226(4)	Mn4–O10	2.089(4)
Mn4–O14	2.221(4)	Mn4–O17	2.105(4)
Mn4–O21	2.209(4)	Mn4–N4[h]	2.309(5)
Mn3–O2	2.232(3)	Mn3–O11	2.128(4)
Mn3–O15	2.228(4)	Mn3–O19	2.109(4)
O1–Mn1–O4	90.33(14)	O16–Mn2–N5[f]	81.69(14)
O1–Mn1–O15	94.01(13)	N3–Mn2–N5[f]	90.03(15)
O1–Mn1–O20	88.73(14)	O6–Mn5–O8	90.66(14)
O1–Mn1–N7[b]	175.98(15)	O6–Mn5–O9	3.68(13)
O1–Mn1–N9[c]	86.38(14)	O6–Mn5–O13	3.02(14)
O4–Mn1–O15	92.88(14)	O6–Mn5–N1	1.19(14)
O4–Mn1–O20	174.11(15)	O6–Mn5–N10[g]	74.16(14)
O4–Mn1–N7[b]	88.17(15)	O8–Mn5–O9	175.62(15)
O4–Mn1–N9[c]	88.78(15)	O8–Mn5–O13	0.76(14)
O15–Mn1–O20	92.98(13)	O8–Mn5–N1	8.72(15)
O15–Mn1–N7[b]	89.79(14)	O8–Mn5–N10[g]	8.85(15)
O15–Mn1–N9[c]	178.29(15)	O9–Mn5–O13	9.53(14)
O20–Mn1–N7[b]	92.39(15)	O9–Mn5–N1	0.66(15)
O20–Mn1–N9[c]	85.36(15)	O9–Mn5–N10[g]	6.88(15)
N7[b]–Mn1–N9[c]	89.86(15)	O13–Mn5–N1	75.76(15)
O2–Mn2–O3	90.75(13)	O13–Mn5–N10[g]	1.17(14)
O2–Mn2–O12	87.70(13)	N1–Mn5–N10[g]	4.61(15)
O2–Mn2–O16	99.90(13)	O6–Mn4–O10	4.77(14)
O2–Mn2–N3	88.51(14)	O6–Mn4–O14	3.07(13)
O2–Mn2–N5[f]	176.16(14)	O6–Mn4–O17	93.62(14)
O3–Mn2–O12	177.60(15)	O6–Mn4–O21	85.08(14)
O3–Mn2–O16	88.63(14)	O6–Mn4–N4[h]	170.47(17)
O3–Mn2–N3	89.46(15)	O10–Mn4–O14	89.18(14)
O3–Mn2–N5[f]	92.78(15)	O10–Mn4–O17	170.35(15)
O12–Mn2–O16	93.44(14)	O10–Mn4–O21	90.60(15)
O12–Mn2–N3	88.68(15)	O10–Mn4–N4[h]	84.86(15)
O12–Mn2–N5[f]	88.73(15)	O14–Mn4–O17	96.55(14)
O16–Mn2–N3	171.40(15)	O14–Mn4–O21	168.10(14)
O14–Mn4–N4[h]	106.43(17)	O14–Mn6–O18	85.68(13)
O17–Mn4–O21	85.39(15)	O14–Mn6–N8[d]	86.16(14)
O17–Mn4–N4[h]	86.07(15)	O14–Mn6–N6[i]	169.80(14)
O21–Mn4–N4[h]	85.40(17)	O18–Mn6–N8[d]	91.50(15)
O2–Mn3–O11	92.92(14)	O18–Mn6–N6[e]	86.89(16)
O2–Mn3–O15	83.40(13)	N6[e]–Mn6–N8[d]	87.05(15)
O2–Mn3–O19	87.69(14)	O2–Mn3–O22	167.12(14)
O2–Mn3–N2[a]	108.71(17)	O11–Mn3–O15	98.71(14)
O11–Mn3–O19	166.58(15)	O11–Mn3–O22	89.01(15)
O11–Mn3–N2[a]	84.59(15)	O15–Mn3–O19	94.68(14)
O15–Mn3–O22	83.72(14)	O15–Mn3–N2[a]	167.37(17)
O19–Mn3–O22	93.39(15)	O19–Mn3–N2[a]	82.53(15)
O22–Mn3–N2[a]	84.15(17)	O5–Mn6–O7	86.35(14)
O5–Mn6–O14	101.42(13)	O5–Mn6–O18	92.38(14)
O5–Mn6–N8[d]	171.72(15)	O5–Mn6–6[e]	5.86(14)
O7–Mn6–O14	94.92(13)	O7–Mn6–O18	78.68(14)
O7–Mn6–N8[d]	89.72(15))	O7–Mn6–N6[e]	2.66(15)
Mn2–O2–Mn3	105.83(14)	Mn5–O6–Mn4	110.79(15)

Note. Symmetry codes: [a] $1/2 - x, 1/2 + y, 1/2 - z$; [b] $-1 + x, y, z$; [c] $-1/2 + x, 3/2 - y, 1/2 + z$; [d] $1 + x, y, z$; [e] $1 - x, 2 - y, -z$; [f] $-1/2 + x, 3/2 - y, -1/2 + z$; [g] $1 - x, 2 - y, 1 - z$; [h] $3/2 - x, -1/2 + y, 1/2 - z$

(Fig. 1). Within each $[Mn_3(isonicotinate)_5(H_2O)]^+$ building block, there are two different isonicotinate bridging modes: two isonicotinate groups adopt an *exo*-tetradentate bridging mode (with a μ_3,η^1,η^2-carboxylato bridge) and orient along the *a* axis, while the other three isonicotinate groups adopt an *exo*-tridentate bridging mode (with a μ_2,η^2-carboxylato bridge) and lie in the *bc* plane. The five isonicotinate groups in each $[Mn_3(isonicotinate)_5(H_2O)]^+$ building block thus provide 17 binding sites, and with one coordinated water molecule, all the Mn centers in **1** adopt six-coordinate, distorted octahedral geometry. The three Mn(II) centers in each $[Mn_3(isonicotinate)_5(H_2O)]^+$ building block form a roughly isosceles triangle. The Mn1–Mn3 and Mn2–Mn3 separations are 3.64 and 3.69 Å, respectively, while the Mn1–Mn2 separation is 4.35 Å. The Mn–Mn–Mn angles for the roughly isosceles Mn1–Mn2–Mn3 triangle are $\sim 53^\circ$ and $\sim 73^\circ$, respectively. The shorter sides of the isosceles triangle (Mn1–Mn3 and Mn2–Mn3) are bridged by one oxygen atom of the μ_3,η^1,η^2-carboxylate group and by two η^2-carboxylate groups in a *syn–syn* conformation. The longer side of the isosceles triangle (Mn1–Mn2) is bridged by one η^2-carboxylate group in a *syn–syn* conformation and by two η^2-carboxylate groups in a *syn–anti* conformation. The roughly isosceles triangle formed by Mn4, Mn5, and Mn6 atoms have essentially the same metrical parameters as those of the Mn1–Mn2–Mn3 triangle (cf., the separations are 3.62, 3.65, and 4.35 Å for Mn5–Mn6, Mn4–Mn6, and Mn4–Mn5 sides, respectively).

At first glance, the 3D extended network structure of **1** seems to be extremely complex, but in fact **1** exhibits a highly regular pillared structure. The isonicotinate groups in the *bc* plane bridge two crystallographically inequivalent $[Mn_3(isonicotinate)_5(H_2O)]^+$ building blocks to form a 2D sheet with *pseudo*-trigonal symmetry (Fig. 2). The adjacent rows in the *pseudo*-trigonal sheet are composed of different $[Mn_3(isonicotinate)_5(H_2O)]^+$ building blocks (i.e., Mn1, Mn2, and Mn3 *vs* Mn4, Mn5, and Mn6). The *exo*-tetradentate isonicotinate groups along the *a* axis serve as pillars to link adjacent *pseudo*-trigonal sheets to form an extended 3D coordination network (Fig. 3). Pillared hydrogen-bonded networks have been previously reported by Ward *et al.* (9). The adjacent *pseudo*-trigonal sheets are rotated 180° and displaced by ~ 2.94 Å from each other along the *b* axis (10). Interestingly, a space filling model viewed down the *b* axis reveals that rectangular channels of $\sim 3.1 \times 4.0$ Å are clearly evident in **1** (Fig. 4). These channels are occupied by perchlorate anions and disordered water and ethanol guest molecules.

TGA studies indicated that **1** experienced a weight loss of $\sim 11.0\%$ in the 30–180°C temperature range. A similar weight loss (10.7%) was achieved by subjecting a pristine sample of **1** to a 10^{-2} Torr vacuum for 24 h. This weight loss corresponds to the complete removal of all the water and ethanol guest molecules as well as coordinated water mol-

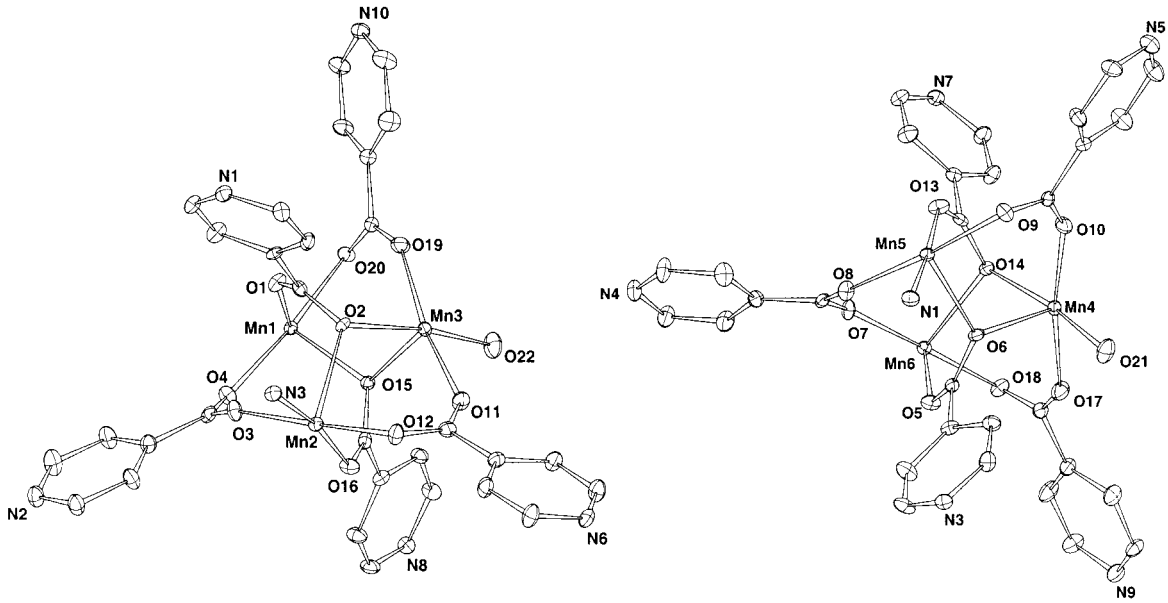

FIG. 1. An ORTEP view of the asymmetric unit of **1** at 50% probability. For clarity, the two crystallographically inequivalent $[Mn_3(isonicotinate)_5(H_2O)]^+$ building blocks are shown separately. The perchlorate anions, the included water and ethanol molecules, and all the hydrogen atoms have been omitted.

ecules (Calcd. 9.43%). Interestingly, an X-ray powder diffraction pattern taken on the sample immediately after evacuating under vacuum indicated that the resulting nanoporous solid maintained the framework structure of **1** (Fig. 5). We have thus obtained a highly regular pillared 3D coordination network that contains rectangular channels.

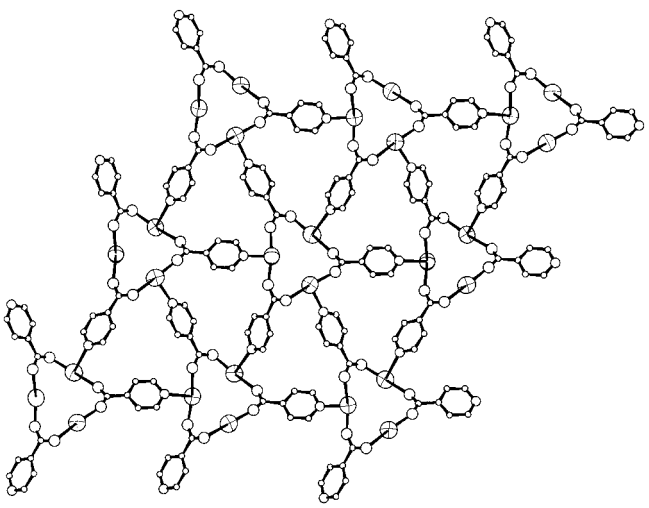

FIG. 2. The *pseudo*-trigonal 2D sheet formed by the Mn(II) centers and *exo*tridentate isonicotinate groups in **1** as viewed down the a axis. The ellipsoids represent the Mn centers, while the circles with increasing sizes represent C, N, and O, respectively.

A qualitative analysis with PLATON shows that the nanoporous solid obtained by evacuation of **1** contains 31.5% solvent-accessible volume (after excluding the volume occupied by the perchlorate anions) (11). TGA analysis also indicated that the evacuated sample of **1** quickly absorbed water vapor from the air within hours.

We have also examined the magnetic properties of **1** at 100 G by SQUID magnetometry. The data at room temperature indicate the presence of three uncoupled, $\mathbf{S} = 5/2$, manganese(II) centers per trimanganese cluster (Fig. 6). The downturn at lower temperature has been modeled adequately utilizing the equation of Kambe for a cluster of three, carboxylate-bridged, high spin Fe(III) atoms (12). Utilizing this model, we are assuming that the present Mn_3 magnetic system is arranged in an isosceles triangle with two intracluster coupling constants, J_S and J_L (representing the coupling constants for short and long sides of the isosceles triangle, respectively), and one g factor. Given that the two crystallographically independent Mn_3 cores have essentially identical metrical parameters, we further assume that they have the same coupling constants and g factor. The Hamiltonian is thus given by

$$H = -J_S(S_A \cdot S_B + S_A \cdot S_C) - J_L \cdot S_B \cdot S_C.$$

Nonlinear least squares fit to two independent data sets from two separate preparations gives $J_S = -3.04 \pm 0.05$ K, $J_L = -4.91 \pm 0.05$ K, and $g = 2.18 \pm 0.05$. The

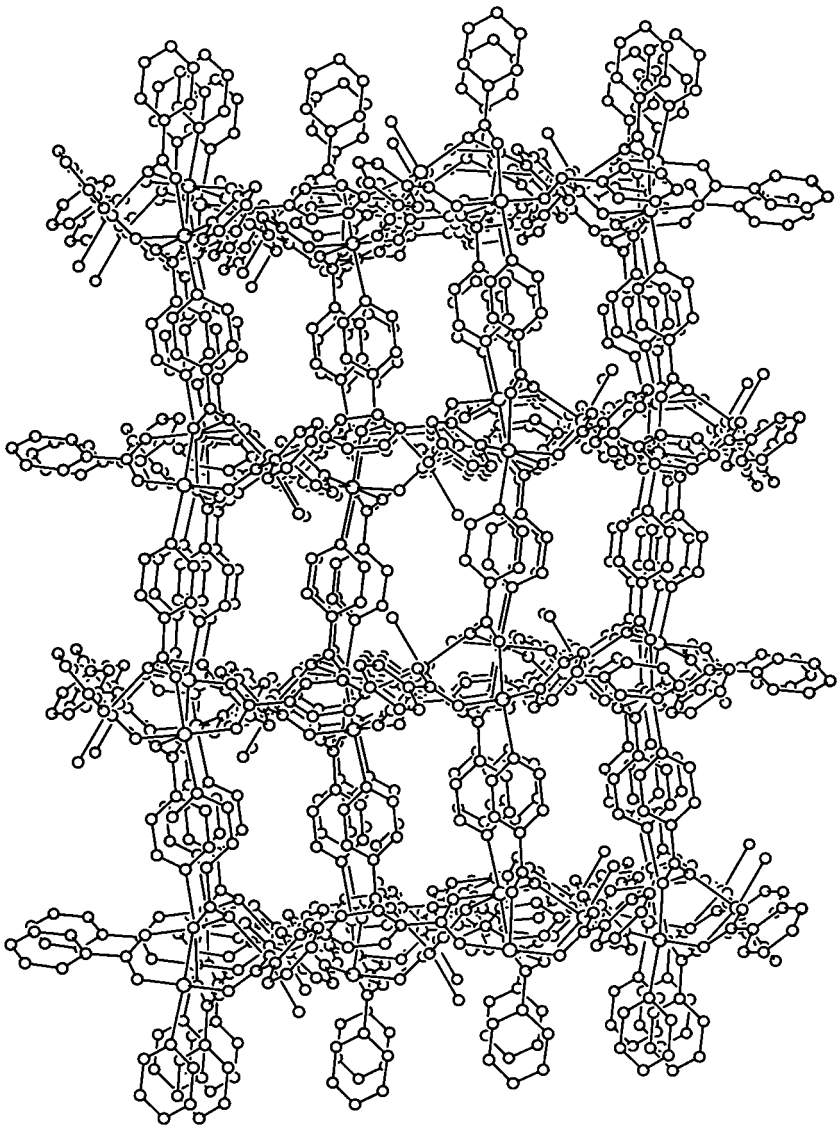

FIG. 3. A perspective view of the pillared 3D network down the *c* axis. The *exo*-tetradentate isonicotinate groups along the vertical directions serve as pillars.

sign and magnitude of J's are consistent with the expected weak antiferromagnetic coupling mediated by the bridging carboxylate ligands and the coupling constants fall within the range observed for other carboxylate-bridged Mn(II)–Mn(II) systems (13, 14). However, the relative magnitude of J_S and J_L seems to be contradictory to the Mn–Mn distances, i.e., the shorter Mn–Mn separations have a smaller coupling constant than the longer Mn-Mn separation. A more careful examination reveals that the observed coupling constants are entirely consistent with the structural features of the $[Mn_3(\text{isonicotinate})_5(H_2O)]^+$ building block. It is well established that the μ_2,η^1-carboxylato bridge is much less efficient in mediating magnetic coupling than the μ_2,η^2-carboxylato bridge and the antiferromagnetic coupling constants of μ_2,η^2-carboxylate-bridged Mn(II)–Mn(II) systems are proportional to the number of the carboxylate bridges (14). In the present Mn_3 system, a superexchange mechanism is clearly operative. Because the longer Mn–Mn separation has three μ_2,η^2-carboxylato bridges while the shorter Mn–Mn separations have only two μ_2,η^2-carboxylato bridges, it is entirely reasonable for J_L to be slightly greater than J_S.

In summary, we have synthesized an unprecedented pillared 3D Mn(II) coordination network based on carboxylate-bridged trimanganese cores. This 3D Mn(II) coordination network contains rectangular open channels

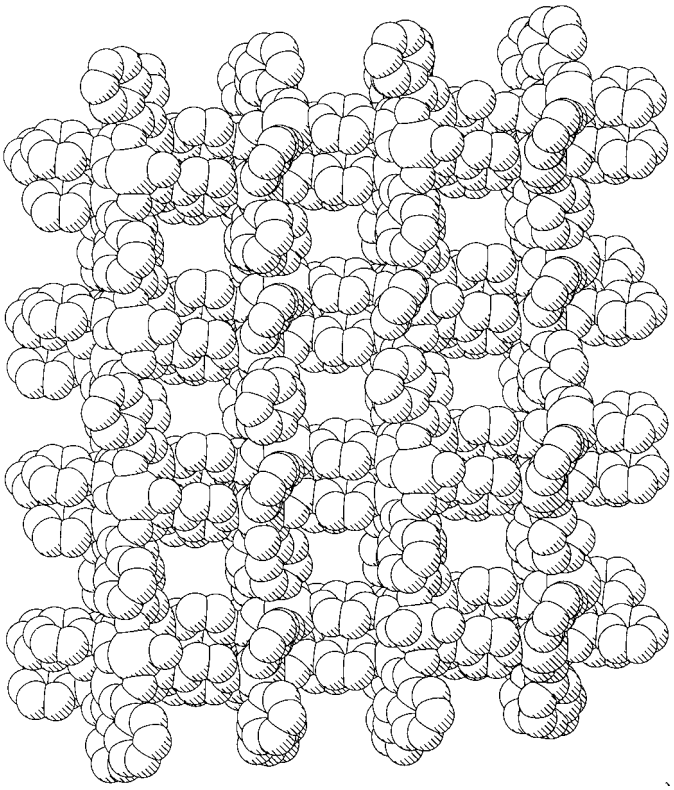

FIG. 4. A space-filling model of **1** as viewed down the *b* axis. Rectangular open channels with a size of $\sim 3.1 \times 4.0$ Å are clearly visible.

that are occupied by perchlorate anions and disordered solvent molecules. These solvent molecules and coordinated water molecules can be readily removed under vacuum at room temperature to afford a nanoporous solid that maintains the framework structure of **1**. As expected, the magnetic interactions between the Mn(II) centers within each carboxylate-bridged trimanganese core are antiferromagnetic in nature.

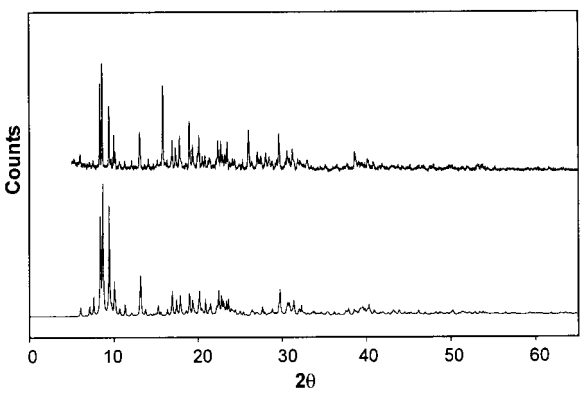

FIG. 5. X-ray powder diffraction patterns of **1**: (bottom) before evacuation, (top) after evacuation.

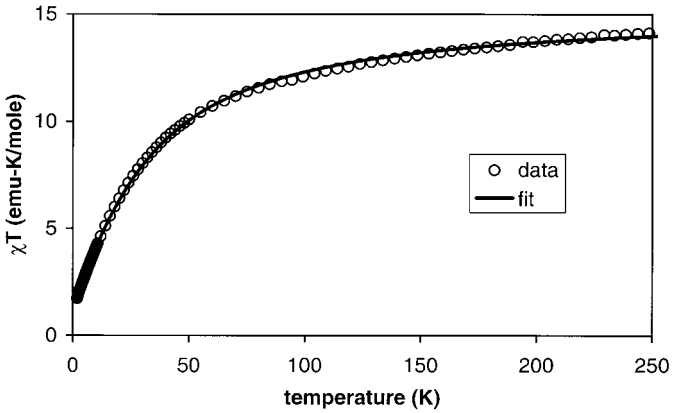

FIG. 6. Plot of χT vs T measured at 100 G. The χT values are per mole of Mn_3 formula units.

ACKNOWLEDGMENTS

We acknowledge financial support from the National Science Foundation (CHE-9727900 and DMR-9875544 to W.L.; CHE-9727485 to G.T.Y.). We thank Dr. Scott R. Wilson and the Materials Chemistry Laboratory of University of Illinois for the collection of X-ray diffraction data. We also thank Dr. Ren-Gen Xiong for help with initial experiments.

REFERENCES

1. (a) J.-M. Lehn, "Supramolecular Chemistry: Concepts and Perspectives," VCH, New York, 1995; (b) C. Janiak, *Angew. Chem. Int. Ed.* **36,** 1431 (1997); (c) O. M. Yaghi, H. Li, C. Davis, D. Richardson, and T. L. Groy, *Acc. Chem. Res.* **31,** 474 (1998); (d) S. R. Batten and R. Robson, *Angew. Chem. Int. Ed.* **37,** 1460–1494 (1998).
2. (a) O. M. Yaghi, G. Li, and H. Li, *Nature* **378,** 703 (1995); (b) T. M. Reineke, M. Eddaoudi, M. O'Keeffe, and O. Yaghi, *Angew. Chem. Int. Ed.* **38,** 2590 (1999); (c) Y.-H. Kiang, G. B. Gardner, S. Lee, Z. Xu, and E. B. Lobkovsky, *J. Am. Chem. Soc.* **121,** 8204 (1999); (d) O. R. Evans, Z. Wang, R.-G. Xiong, B. M. Foxman, and W. Lin, *Inorg. Chem.* **38,** 2969 (1999); (e) G. B. Gardner, D. Venkataraman, J. S. Moore, and S. Lee, *Nature* **374,** 792 (1995); (f) C. J. Kepert and M. J. Rosseinsky, *Chem. Commun.* 31 (1998); (g) S. R. Batten, B. F. Hoskins, and R. Robson, *Angew. Chem. Int. Ed. Engl.* **36,** 636 (1997); (h) O. M. Yaghi, C. E. Davis, G. Li, and H. Li, *J. Am. Chem. Soc.* **119,** 2861 (1997).
3. (a) L. Quahab, *Chem. Mater.* **9,** 1909 (1997); (b) G. Mislin, E. Graf, H. W. Hosseini, A. Bilyk, A. K. Hall, J. M. Harrowfield, B. W. Skelton, and A. H. White, *Chem. Commun.* 373 (1999); (c) J.-M. Lehn, *Angew. Chem. Int. Ed. Engl.* **27,** 89 (1988).
4. R. E. Newnham, "Structure-Property Relations," Springer-Verlag, New York, 1975.
5. (a) W. Lin, O. R. Evans, R.-G. Xiong, and Z. Wang, *Z. J. Am. Chem. Soc.* **120,** 13272 (1998); (b) O. R. Evans, R.-G. Xiong, Z. Wang, G. K. Wong, and W. Lin, *Angew. Chem. Int. Ed. Engl.* **38,** 536 (1999).
6. G. M. Sheldrick, *Acta Crystallogr A.* **46,** 467 (1990).
7. G. M. Sheldrick, "SHELXS-97, Program for Crystal Structure Refinement," Universität Göttingen, Germany, 1997.
8. R. G. Xiong, S. R. Wilson, and W. Lin, *J. Chem. Soc. Dalton Trans.* 4089 (1998).
9. (a) V. A. Russell, C. C. Evans, W. Li, and M. D. Ward, *Science* **276,** 575 (1997); (b) J. A. Swift, A. M. Pivovar, A. M. Reynolds, and M. D. Ward, *J. Am. Chem. Soc.* **120,** 5887 (1998).
10. This displacement is defined as half the projected distance between the tips of the two Mn_3 triangles.
11. P. v.d. Sluis and A. L. Spek, *Acta Crystallogr A* **46,** 194 (1990).
12. K. Kambe, *J. Phys. Soc. Jpn.* **5,** 48 (1950).
13. S. Menage, S. E. Vitols, P. Bergerat, E. Codjovi, O. Kahn, J.-J. Girerd, M. Guillot, X. Solans, and T. Calvet, *Inorg. Chem.* **30,** 2666 (1991).
14. H. Ikura and T. Nagata, *Inorg. Chem.* **37,** 4702 (1998).